

Brain Computer Interface For Mobility- A Case Study With ALS Patient

D.Hari Krishna, Rakesh Sengupta, I.A.Pasha and T.Satya Savithri

Abstract

The aim of this paper is to explore different classification algorithms in classifying an EEG signal acquired from ALS and normal subject by conducting motor imagery based BCI system experiment and P300 based temporal oddball experiment. We also tested the performance of the these classifiers in moving a robotic wheel chair from one point to another in shortest path using optimal path planning algorithm. The results of the classification accuracy and time taken by different classifiers are presented. The system is useful for ALS patients in moving from one location to another location in indoor environment.

Index Terms—BCI, ALS, Motor Imagery, cross correlation.

Introduction

Advances in biomedical signal processing, especially the EEG signal, and mobile robot control have allowed the development of robotic wheelchairs commanded by BCI [1-2]. Such vehicles use some EEG characteristics, such as potentials from an imaginary motor task or evoked potentials in the development. By integrating BCI features and autonomous robot capabilities with normal wheel chair, we can get the useful assistive device. This is helpful for people who are paralyzed, and are unable to control parts of their body as much as necessary to activate the joystick of a robotic wheelchair. Many people can use this to gain autonomy, and to avoid a helper to move their wheelchair in a controlled environment indoors. With the new system, the ALS patient sits in the wheelchair and thinks about the direction they want to move. When people concentrate on a desired direction, their brains start emanating P300 waves because attention is deployed in those directions more than others. Even the desire for a movement can be recorded as event-related de-synchrony (ERD) in the EEG signal. These are promptly recorded by an EEG machine which sends the controller in the desired direction. This paper presents two approaches for wheel chair navigation: i. Motor imagery based navigation ii. P300 based oddball paradigm. For autonomous robotic systems, it is also essential to detect and avoid the obstacles in its path as well as to make its own decisions in the path planning.

while moving from source to the destination. Several path planning techniques have been developed for mobile robots [3-5]. These techniques depend on different environments and types of sensors etc, and these approaches help to improve performance in terms of time, distance, cost and complexity. There are three subtasks in the robot navigation problems - a) mapping and modeling the environment, b) path planning, and c) path traversal with collision avoidance [6]. In the current work we designed a control system using A-star/Dijkstra path planning algorithm

In the present paper, Section 2 describes about i) Motor imagery based BCI system experiment ii) P300 based temporal odd ball paradigm experiment in which data collection, data analysis (pre-processing, feature extraction and feature classification) steps are involved. Section 3 discusses in detail the path planning algorithm. Section 4 elaborates the proposed control system configuration and finally section 5 about conclusion of the proposal.

Experiment Details

Motor Imagery based BCI System

In motor imagery based BCI paradigm, subjects have to imagine performing a specific motor action (e.g. clenching hand or rotating foot) without any external motor movement. We then classify the patterns in the electro encephalogram signal (EEG) with the help of feature extraction and classification into useful commands to be given to an external device. In this way the EEG signals can be used as feedback for motor disabled patients to communicate with the external environment.

We employed EEG machine mainly consisting of master controller and type-D EEG amplifier. During the experiment, a 24 electrode EEG cap is placed on the scalp with a conductive gel to record the activity of the brain cells. Recording these voltages over time gives us the EEG. Signal received from EEG cap will be amplified by EEG amplifier before transmitting to EEG controller as the original EEG signal was having very modest amplitude in the order of μV . Master Controller is the control station of the system, coordinating the inputs from the ERP stimulator and the EEG amplifier.

Generally EEG signals are Multi channel Time series evaluations that are indicators of the underlying the brain activity. The channels are most often not independent and often there is a high degree of correlation between different channels in EEGs and they are very noisy. Due to the characteristics of signal periodicity we can separate the EEG signal from noise and we can use it to measure the degree of similarity between two signals in time.

We conducted the motor imagery (MI) experiments where subjects imagined movements of Right hand, right leg, left leg and left hand for 256 trials (each trial length: 4 sec) on a Normal subject as well as ALS patient (Figures 1 and 2). The system first instructs the subject by showing the visual display that indicates to the subject which MI task has to be performed. Figure 1a and 1b show how the visual displays are given. After each imagined movement subject has to relax for 4 sec. Then EEG signals are recorded from the 24 channels which are placed on the top of the cap.



Figure 1: MI Experiments conducted on a) ALS Patient b) Normal subject right hand MI visual feedback

Cross correlation technique for the features extraction

To analyze and classify the Motor imagery data we proposed two algorithms CC-SVM and CC-LDA which are a combination of cross correlation for feature extraction [7] and SVM/LDA for classification. The Cross Correlation of two signals is obtained by multiplying corresponding ordinates and summing for all portions of the signals within a time window. Cross correlation follows three steps to extract the features from the given set of data: 1) random selection of one of the EEG channels as a reference channel 2) cross-correlate the reference channel with the remaining data channels 3) calculate the six statistical features (mean, median, mode, standard deviation, maximum and minimum) from each cross-correlation sequence to reduce the dimensions [8].

$$R_{xy}[m] = \sum_{i=0}^{N-|m|-1} x[i]y[i-m]; m = -(N-1), -(N-2), \dots, (N-2), (1)$$

$R_{xy}(m)$ is the cross-correlated sequence at m lag. If each of the signals, x and y , consists of M finite number of samples, the resultant cross-correlation sequence has $2M-1$ samples. If x and y are not the same length, for example, x and y have N and M number of samples, respectively, and if $N > M$, the resultant cross-correlation sequence has $(2N-1)$ number of samples. The shorter vector, here y , is zero-padded to the length of the longer vector, x .

Here we chose the Fp1 as reference channel for the Right hand MI task as there is no specific selection criterion in the Cross Correlation system. As mentioned before, there are 24 channels in each of the two classes of a subject. The reference channel data obtained from the MI experiment performed on the subject is cross-correlated with the data from the remaining 23 channels of the Right Hand class and 24 cross-correlation sequences are obtained for this class. Again, in the Left Leg class of the same subject, the reference channel data is cross-correlated with each of 24 channels data and produces 24 cross-correlation sequences. Thus, a total of 47 cross-correlation sequences are obtained for the two-class MI data for each subject. The results of cross-correlation sequences named as cross-correlograms for the Right Hand and the Left Leg of MI data of subject are plotted as shown in Figure 2. It can be observed that when the test observation matches with the same class we get a spike in the

correlogram (Figure 2), and in case of mismatch class results we cannot identify any significant spike in correlogram.

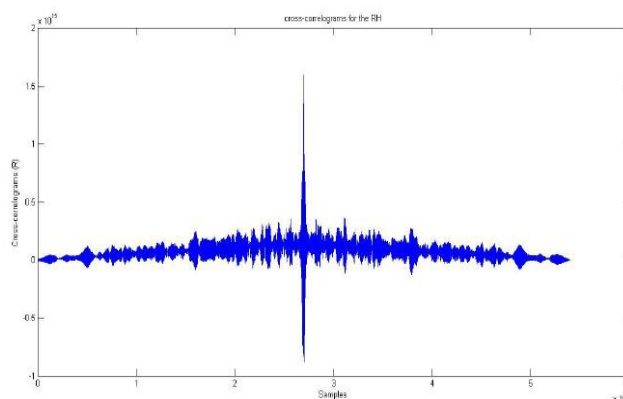


Figure 2: Cross-correlograms for the Right hand

It is important to note that the cross-correlogram or cross-correlation sequences (R_{xy}) are calculated using Eq. (1) for each lag. Finally, we obtain 23 feature vectors of six dimension for six statistical features for subject Right hand and another 23 feature vectors for Left leg.

Cross correlation based classifiers

The feature vectors are fed to LDA and SVM classifiers as inputs to classify the differentiations for given input feature vectors. The classified output emulates the input MI task which can be translated as command for controller system. Here we also calculated the classifier accuracy by cross validation method for our data set. We choose the 3-fold cross validation procedure. The 47 feature vectors of six dimensions are divided into three subsets containing the equal number of observations. Each time, a subset is used as a testing set and the remaining two subsets comprise a training set. The procedure is repeated three times (the folds) with each of the subsets as the test set. Finally the average classification accuracy is evaluated across all the folds, is called the cross validation accuracy.

P300 based temporal odd ball paradigm for BCI system

The P300 wave is an ERP component commonly observed in a variety of phenomena including the decision making process. The user is subjected to events that can be categorized into two distinct categories. One of the category is rarely displayed. The user performs a task that cannot be done without categorization into either one of the categories [9]. Whenever the rare event is displayed it generates a P300 signal. It is a distinct large positive signal that occurs 300 milliseconds after the event onset. The signal is typically measured most strongly by the electrodes covering the parietal lobe. We analyzed Cz electrode, the amplitude of the P300 signal is inversely related to the rate of the rare event presented to the user. Although many P300-BCI systems have

achieved 100% accuracy [2], the problem with this type of BCI is its dependence on the continuous visual attention of the user, which is usually intolerable for locked-in patients who are the most important target for BCI technology - especially if used for a long time. The presence, magnitude and timing of the P300 signal are often used as metrics of cognitive function in decision making processes. In our proposal, we considered the features of P300 to decide whether the subject is interested to move from his/her present position or not based on the classifier response applied to the wheel chair controller.

2.2a Data collection

In behavioral method, we have placed an oddball of variable clock frequency in a temporal sequence of standard stimuli. 4 normal subjects of age between 18 and 21 have participated in the experiment. They were immature with respect to the purpose of the experiment. All had normal or corrected-to-normal vision. The stimuli were presented using a monitor of size 17". The subjects sat at a distance of 66cm from the screen. The standard ball was a black circle with 10mm radius, centered on the screen. The oddball is represented in red color with same size. Both standard and oddball stimuli are presented on a white background. Figure 3 shows different trials of odd ball paradigm stimuli.

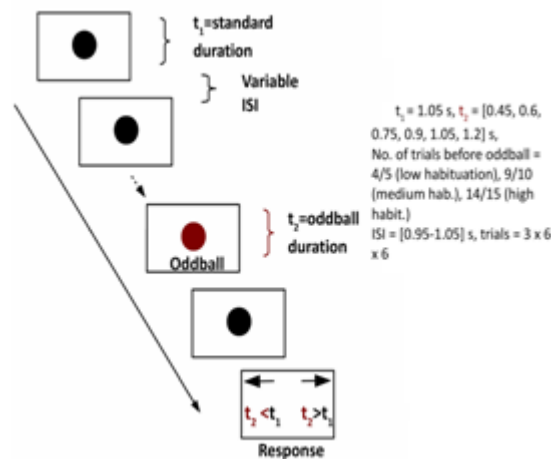


Figure 3: Odd ball paradigm stimuli

The subjects are required to fixate the centre of each standard or oddball as it appears and to maintain fixation on this location between the appearances of successive stimuli throughout the experiment. Each oddball occurred within a train of standard stimuli of constant objective duration. We considered a sequence of 6 balls. The oddball appeared randomly at any position in the sequence.

The sequence of oddball appearance tested within the experiment (Figure 4) were randomized so that the observers could not know when the oddball would appear. A

total of 108 stimuli were presented to the subject which lasted for an average time of 45 minutes. The observers were told that all the standards were of constant duration.

Figure 5 shows that, if the experiment is done in three ways, based on habituation i.e. Six trial experiment, Eleven trial experiment, and Sixteen trial experiment, due to habituation, P300 amplitudes may vary. If habituation is more, the amplitude of P300 is higher as odd ball is more salient. Similarly, if habituation is lesser, amplitude of P300 is lesser because the odd ball does not appear as salient.



Figure 4: Subject performing the odd ball experiment

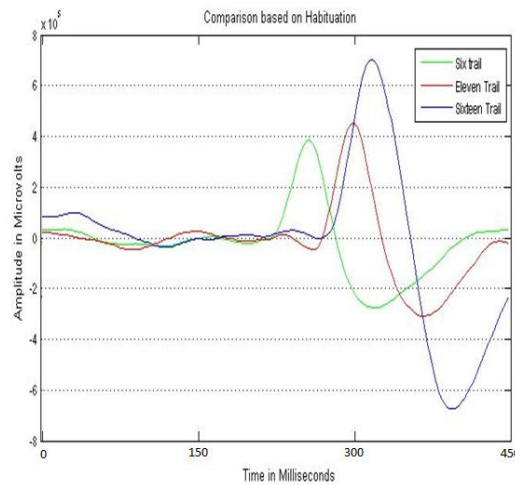


Figure 5: Comparison of P300 amplitudes based on Habituation

Data analysis

Pre Processing

After the collection of data from a 24 electrode EEG machine, the data needs to be processed and analyzed. As we are interested in P300 component, and it is prominent in the central lobe especially at Cz electrode, we consider data at only this electrode for the analysis. In the current montage 20th electrode was the Cz electrode.

Artifact removal

For artifact removal, we use Moving average filter. The moving average is the most common filter in Digital Signal Processing (DSP), mainly because it is the easiest digital filter to understand and use. A moving average is commonly used with time series data to smooth out short-term fluctuations and highlight longer-term trends or cycles. The threshold between short-term and long-term depends on the application, and the parameters of the moving average will be set accordingly. Here we use a window of size 12. Given a series of numbers and a fixed subset size, the first element of the moving average is obtained by taking the average of the initial fixed subset of the number series. Then the subset is modified by shifting forward; that is, excluding the first number of the series and including the next number following the original subset in the series. This creates a new subset of numbers, which is averaged. This process is repeated over the entire data series. The plot line connecting all the (fixed) averages is the moving average. A moving average is a set of numbers, each of which is the average of the corresponding subset of a larger set of datum points.

The plot of the data before & after passing through moving average filter is shown in Figure 6.

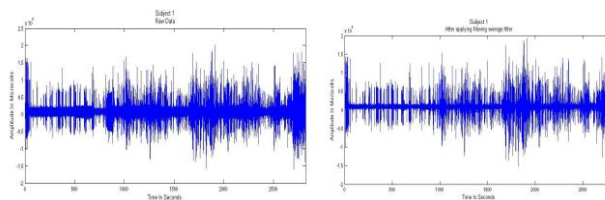


Figure 6: (a) Data before (b) after passing through moving average filter

Basic noise removal

After filtering the data using Moving Average, the data is passed through the 50Hz Notch filter to remove the noise due to AC. Notch filter is a band-stop filter with a narrow stop band (high Q factor). **Extraction of epoch**

After removing the noise and artifacts from the data, the epochs are to be extracted. These epochs require very detailed time stamps, i.e. time of starting and ending of every event occurred during the experiment. The experiment contains 2 kinds of epochs, one is epoch for a standard ball (black ball) and the other is for an odd ball (red ball). For each trial there is one odd ball, so there are 108 odd stimuli and the rest are normal balls for one subject. The plot of the extracted odd ball epochs are shown in Figure 7.

Features Extraction

In general, it is very simple to classify similar objects in the same class, and two different classes can be distinguished according to their differences. In order to identify the class of a given object, we need to extract some properties which can reflect the similarities in the same class as well as differences between classes. In our proposal, we considered the features Root Mean Square (RMS) amplitude and band powers of the extracted epochs for classification.

Calculating RMS amplitudes for extracted epoch

After the epoch extraction, the RMS amplitudes of the epochs are to be found out which is one of the essential feature. The RMS values are essential as they determine the amplitudes of P300 in the epochs.

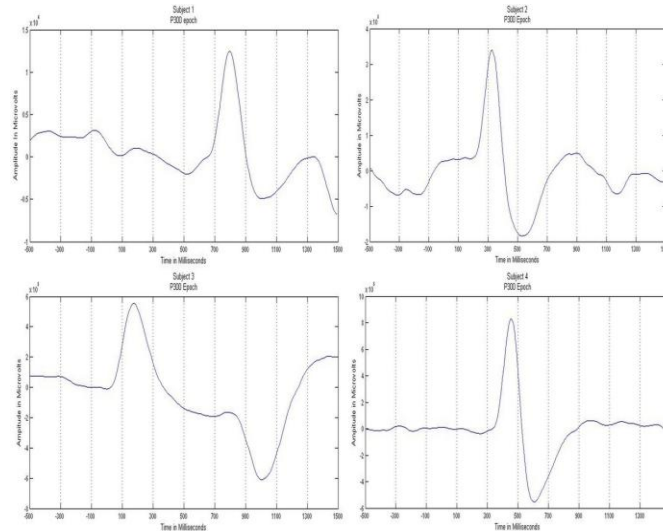


Figure 7: Odd ball epoch showing P300

RMS values are higher for the epochs which contain P300 and lesser for the others, for a fairly noise less data.

Extraction of band powers for the epoch

There are 7 bands, i.e. Delta (0.5-4Hz); Theta (4.5-8Hz); Alpha1(8.5-11Hz); Alpha2 (11.5-14Hz); Beta1 (14.5-25Hz); Beta2 (25.5-35Hz); Gamma (33.5-50Hz). After the band pass filtering, the filtered signal is passed to a module which finds the band power of the given signal. Here the length in seconds of the epoch and the epoch are to be given as inputs. There are seven band powers for each epoch. These also play a vital role as they are also used to differentiate the P300 epochs from non-P300 epochs.

The delta and theta are the two most prominent frequency bands in continuous attention tasks. There are some common ways to calculate band powers, such as band pass filtering and squaring the samples; using Fast Fourier Transformation (FFT) to transform the signal weighted by a Hamming window to the frequency domain and to calculate the signal power in the frequency band of interest. Compared to FFT method, the first method retains amplitude but ignores phase information.

If the Fourier coefficients are denoted as $X_v = a_v + jb_v$, and the resolution of the FFT as Δf , the phase $\Psi = \tan^{-1}(b_v/a_v)$ and the amplitude $A = |X_v|$.

The power in the frequency bands are given by Eq. (2) and (3)

$$P_{\Delta} = \sum_{V|\Delta f \leq 0.5\text{HZ}} [X_V]^2 \quad (2)$$

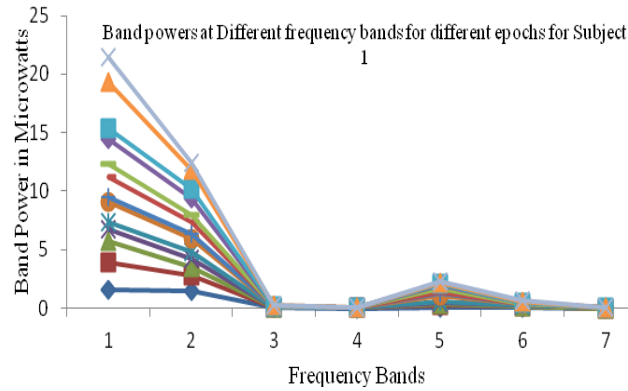


Figure 8: Band powers at different frequency bands for different epochs

$$P_{\theta} = \sum_{V|\Delta f \leq 0.5\text{HZ}} [X_V]^2 \quad (3)$$

Here Δf was set to 0.5Hz. A study [10] reports that phase information can be combined with band powers to achieve better performance, but in our case no improvement was found, hence not used further.

All these features are concatenated into a single feature file. The Band powers for each epoch in each band designated in sub Section g above are given in Figure 8. Here, we can observe that there is a significant change in band powers from Delta to Theta band. Also it indicates that band power is more prominent in that band.

P300 Classification

After features extraction, the features form the primary data are sent for classification. Here these features are divided into two classes or groups, one group which has P300 and other which doesn't. The classification is done based on the training data. The training data is the already classified data given as input to the classifier code. This classifier returns weights, depending on the feature values and their classes. For our experiment, we used 80% of data for training and 20% for testing. The features need to have labels for the training purpose.

There are two types of labels, as there are two types of classes. Labels are taken as 1 and -1. The training data and the labels are given as inputs for the classifier. For the offline analysis of whole data, we considered the best standard classifiers. The accuracy of the classification depends on the features included for classification, the number of features and the classifier. Considering these factors, we have three of the best standard offline classifiers, they are LDA, SVM and D-LDA [11].

Classification Results

Figure 9 gives classification accuracies of different classifiers in MI experiment. It can be observed that CC-SVM classifier results in high accuracy (99.76% & 97.9%) for both neurotypical and ALS subjects compared to CC-LDA (60.04% & 41.7%).

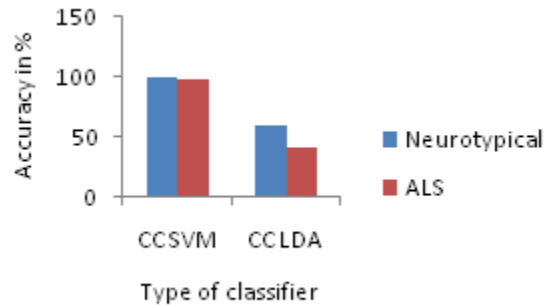


Figure 9: Performance of the classifiers for two subjects in MI

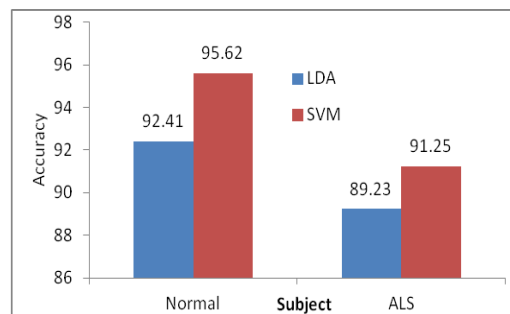


Figure 10: Classifier accuracy in P300 based BCI

Similarly figure 10 gives classification accuracies of different classifiers in P300 based BCI experiment. Again it can be observed that SVM classifier results in high accuracy (95.62% & 91.25%) for both normal and ALS subjects compared to LDA (92.41% & 89.23%).

Figure 11 shows that SVM classifier takes more time for classification (4.1secs) when compared to LDA classifier. This drawback is ignored in the offline analysis as the response time is of no importance in moving a robotic wheel chair from one point to another point.

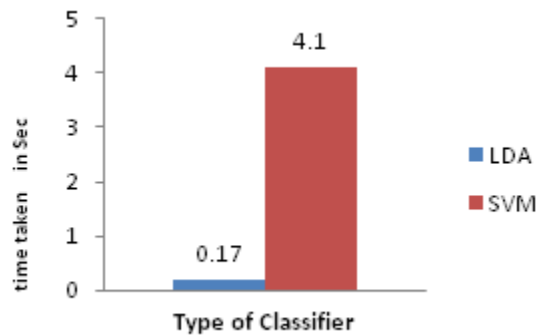


Figure 11: Time taken by Different classifiers in P300 based BCI

Path Planning Of Controller Using Modified A-Star Algorithm

Modified A-Star algorithm for path planning: In A-star algorithm shortest path between two points is decided by calculating F score for each cell in the map. Here F score can be calculated from the formulae $F=G+H$, where G represents the moment cost from one cell to its adjacent cell either in horizontal, vertical or in diagonal directions starting from source until it proceeds to the end point. H represents the distance between the present cell and the goal node in terms of number of cells. The shortest path can be the one with least F scores between the starting and goal nodes. The process of calculating the F score and choosing the path with least F score will be repeated until the target node is added to the closed list and open list is to be cleared.

Obstacle avoidance: In our proposed control system we consider two obstacle problems *i. Static obstacle, ii. Dynamic obstacle.*

Table 1: Rotational angle correction of wheel chair for direction change

Directions/Node Location(deg)	Row	Column
Same Row	Same Row	Column+1
Right/+90	Row+1	No change
Left/-90	Row-1	No change
Front diagonal right/+45	Row+1	Column+1
Front diagonal left/-45	Row-1	Column+1
Back diagonal right/+135	Row+1	Column-1
Back diagonal left/-135	Row-1	Column-1
Back/-180	Same Row	Column-1

obstacle is encountered along the path then the wheel chair redefines its path based on one of the two obstacle avoidance methods as discussed above. Before remapping the path plan on detection and avoidance of dynamic obstacle; the wheel chair resets its direction by calculating the error angle between the source node and present node, where it encountered obstacle. For example, Direction angle of wheel chair at node A in Fig. 12b is $x_1=0$ deg and the error angle between nodes A and A1 is $x_e=x_1+x_2=0+90$. The wheel chair rotates 90 degrees in anticlockwise to attain its reference position as at A before remapping the optimized path. The similar procedure will be followed to estimate error angle between the nodes in all directions i.e. front left (FL), front (F), front right (FR), left (L), right (R), back left (BL), back (B) and back right (BR) as in Fig. 13b on obstacle detection before remapping the path.

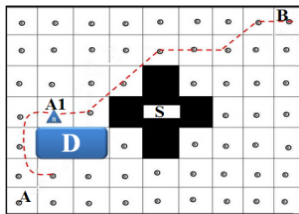


Figure 13a: Remap path after dynamic obstacle avoidance

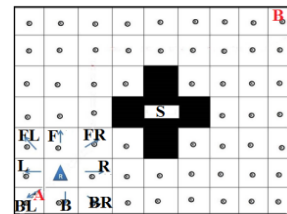


Figure 13b: Rotational angle calculation of wheel chair for direction change

In the path construction 2 the wheel chair avoids the obstacle using boundary follow method as in Fig. 13a. When avoidance is finished it adjusts its direction angle to reference direction angle and reads its current cell position by RFID reader to make new source point. Again a new path planning is done for the new source point and the goal point to continue the moment from the reset location. The MI based BCI was tested with a healthy subject. The user interface display has choices designated by Point-A, Point-B. Now each MI task is assigned to one of the two choices. For example if the user intends to move to destination Point-A from source point-B, the user has to perform RH MI-task. The features are extracted from the correlograms corresponding to every MI task. Then the CC-SVM classifier translates the features into controlling commands and applies to the controller. National Instruments robotic starter kit 2.0 with SBRIO-9632 is used to implement the control system navigation based on MI commands. The known environment in the presence of static obstacles is converted into occupancy grid map of 1mx1m and assigned RFID tags for each cell for cell identification. With the given command, the controller generates a shortest navigation path from prior given occupancy map avoiding the obstacles in each cell until the wheel chair reaches the goal.

Conclusion

As a prototype first we implemented the total control system on National Instruments robotic starter kit 2.0 with SBRIO-9632 by using the offline commands of MI tasks. In experiment1, the known environment is converted into occupancy grid map with static

obstacles and RFID tags are assigned and applied to the robot. In the map robot is at location 'A' as shown in Figure 11. Now the user performed an MI task of Left leg after the completion of all steps which are signal acquisition, cross-correlation and classification a controlling command is generated and applied to the controller of robot then the controller generates a shortest path from prior given occupancy grid map and controls the moment of robot in that direction with the help of RFID tags placed in cells by checking and avoiding the obstacles in each cell as shown in Figure 11 a-d. In the experiment2, we have implemented a wheel chair navigation using the P300 signal attained from an oddball experiment of variable clock frequency in a temporal sequence of standard stimuli. P300 stimulus is produced when the subject intends to move from source to the destination. The current location of the wheel chair will be considered as the source point for the wheel chair. We tested our algorithm as a prototype and implemented the total control system on National Instruments robotic starter kit 2.0 with SBRIO-9632 by using the offline commands of P300 stimulus. First the known environment is converted into occupancy grid map with static obstacles and RFID tags are assigned and applied to the robotic wheel chair.

This novel implementation opens newer possibilities not just towards assistive technologies, but also in terms of cognitive assessment of ALS and quadriplegic patients.

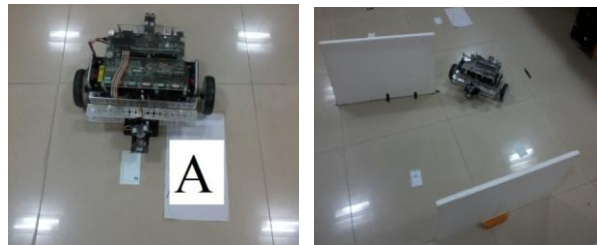


Figure 11: a. Start location from A

Figure 11: b. Path planning

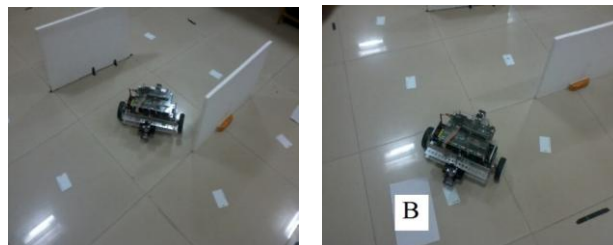


Figure 11: c. Obstacle avoidance

Figure 11: d. End location to B.

Acknowledgment

This work was supported by Department of Science and Technology (DST), Government of India, under the Cognitive Science Initiative (CSI) sponsored project (Ref. No: SR/CSI/133/2011).

References

- [1] Bastos-Filho T F., Cavalieri D C., Celeste W C., Ferreira A., Filgueira P N S., Arantes I B., Martins V R., Silva R L and Sarcinelli-Filho M., 2008, "Case study: Cognitive control of a robotic wheel chair," in *Wearable Robots: Biomechatronic Exoskeletons*, J L Pons (Ed.) New York: John Wiley & Sons, pp 314-322.
- [2] Millán J, Mouriñoand W, Gerstner J, Renkens F, 2004, "Non-invasive brain actuated control of a mobile robot," *IEEE Trans. Biomed. Eng.*, 51(6), pp. 1026-1033.
- [3] Buniyamin N., Wan Ngah W.A.J., Sariff N., Mohamad Z., 2011, "A Simple Local Path Planning Algorithm for Autonomous Mobile Robots," *International Journal of Systems applications, Engineering & development*, 5(2), pp. 151-159.
- [4] Sariff N B., Buniyamin N., 2010, "Ant Colony System For Robot Path Planning In Global Static Environment," in *9th WSEAS International Conference on System Science and Simulation in Engineering (ICOSSSE'10)*, Japan, pp.192-197.
- [5] D.HariKrishna., N.V.Jagadeesh., I.A.Pasha and T.Satya Savithri., 2013, "BCI controller based on imagery activity using shortest path algorithm," in *IEEE Asia Pacific Conference on Postgraduate Research in Microelectronics and Electronics (PrimeAsia)*, India, pp. 68-72.
- [6] Behnke S, 2004, "Local Multi resolution Path Planning," in *7th Robo cup Int. Symposium*, Italy, pp. 332-343.
- [7] Siuly, Li Yan P. Wen, 2013, "Identification of Motor Imagery Tasks through CC-LR Algorithm in Brain Computer Interface," *International Journal of Bioinformatics Research and Applications*, 9(2), pp. 156-172.
- [8] Abdullah H., Maddage N C., Cosic I and Cvetkovic D., 2010, "Cross-correlation of EEG frequency bands and heart rate variability for sleep apnoea classification," *Med Biol Eng Computer*, 48(12), pp. 1261-1269.
- [9] Bogacz R., Usher M., Zhang J and McClelland J.L., 2007, "Extending a biologically inspired model of choice: multialternatives, nonlinearity and value-based multidimensional choice," *Philos. Trans. R. Soc. Lond. B Biol. Sci*, 362 (1485), pp 1655–1670.
- [10] Graimann B., Pfurtscheller G., Townsend G., 2006, "A comparison of common spatial patterns with complex band power features in a four-class BCI experiment," *IEEE Transactions on Bio medical Engineering*, 53(4), pp 642-651.
- [11] Arnaldi B., Congedo M., Lamarche F., Lécuyer A and Lotte F., 2007, " A review of classification algorithms for EEG-based brain-computer interfaces," *Journal of Neural Engineering*, 4(2), pp. R1–R13.

- [12] Choset H., Lynch K.M., Hutchinson. S., Kantor. G., Burgard. W., Kavraki. L. E., Thrun S., 2005, "Principles of Robot Motion: Theory, Algorithms and Implementations," Boston, London: MIT Press.
- [13] Sankaranarayanan. A., Vidyasagar. M., 1990, "Path planning for moving a point object amidst unknown obstacles in a plane: a new algorithm and a general theory for algorithm development in Decision and Control," in *29th IEEE Conference on Decision and Control* Hawaii, pp.1111-1119.
- [14] Claudiu. P., Dupac. M., 2009, "An Optimal Path Algorithm for Autonomous Searching Robots," in *Annals of University of Craiova, Math. Comp. Sci. Ser.*, 36(1), pp. 37-48.